Check for updates

Optics Letters

Quantum cryptography with structured photons through a vortex fiber

Alicia Sit,[1,*] Robert Fickler,[1] Fatimah Alsaiari,[1] Frédéric Bouchard,[1] Hugo Larocque,[1] Patrick Gregg,[2] Lu Yan,[2] Robert W. Boyd,[1] Siddharth Ramachandran,[2] and Ebrahim Karimi[1]

[1]Department of Physics, University of Ottawa, Advanced Research Complex, 25 Templeton Street, Ottawa, Ontario K1N 6N5, Canada
[2]Department of Electrical and Computer Engineering, 8 St. Mary's St., Boston University, Boston, Massachusetts 02215, USA
*Corresponding author: asit089@uottawa.ca

Received 13 June 2018; revised 20 July 2018; accepted 26 July 2018; posted 27 July 2018 (Doc. ID 335026); published 17 August 2018

Optical fiber links and networks are integral components within and between cities' communication infrastructures. Implementing quantum cryptographic protocols on either existing or new fiber links will provide information-theoretical security to fiber data transmissions. However, there is a need for ways to increase the channel bandwidth. Using the transverse spatial degree of freedom is one way to transmit more information and increase tolerable error thresholds by extending the common qubit protocols to high-dimensional quantum key distribution (QKD) schemes. Here we use one type of vortex fiber where the transverse spatial modes serves as an additional channel to encode quantum information by structuring the spin and orbital angular momentum of light. In this proof-of-principle experiment, we show that two-dimensional structured photons can be used in such vortex fibers in addition to the common two-dimensional polarization encryption, thereby paving the path to QKD multiplexing schemes.

OCIS codes: (060.2330) Fiber optics communications; (060.5565) Quantum communications; (270.5568) Quantum cryptography.

https://doi.org/10.1364/OL.43.004108

Implementing quantum cryptography is necessary for improving the security of sensitive information. Following the development of the first quantum key distribution (QKD) protocol by Bennett and Brassard in 1984 (BB84) [1], much progress has been made in transmitting information farther and faster. Experimentally, it is important to investigate realizations of different quantum channels for various real-world scenarios that require the security of quantum cryptography. Free-space channels, in particular between ground stations and satellites, satisfy the need for long distance, global connections where optical fibers are not an option [2–5]. On a shorter length scale, optical fiber quantum channels become favorable as they do not have problems with line-of-sight, weather, or time of day [6]. Indeed, intra-city optical fiber networks have been retrofitted to transmit quantum signals [7], and commercially available fiber systems are now readily available for secure data encryption [8].

In general, a challenge that quantum channels face is the capacity to send more information. One solution is to encode information using multiple photonic degrees of freedom, for example, spin angular momentum (SAM) and orbital angular momentum (OAM). Light carrying OAM possesses a phase term of $e^{i\ell\varphi}$, where ℓ is an integer and φ is the transverse azimuthal coordinate, leading to ℓ helical wavefronts and doughnut-like intensity distributions. The OAM Hilbert space is unbounded, corresponding to a theoretically infinite encoding alphabet [9,10]. In practice, the number of spatial modes that can be transmitted through a quantum channel is constrained by the numerical aperture of the system but, nonetheless, are useful for high-dimensional protocols [11,12]. We refer to photons encoded using multiple photonic degrees of freedom as *structured*, since the coherent combination of SAM and OAM creates spatially varying transverse polarization distributions [13]. Thus, the amount of transmitted information can be doubled for a fixed ℓ. QKD with OAM and structured photons has so far been successfully demonstrated in free space [14–16].

Several varieties of specialty fibers exist that can transmit OAM modes, including vortex or rings [17], twisted photonic crystals [18], inverse-parabolic graded indices [19], and air-core fibers [20,21]. The vortex fibers, characterized by rings of higher refractive indices in their transverse profiles, have been shown to preserve entanglement [22], as well as terabit per second transmission rates through OAM multiplexing in classical communication schemes [23]. Recently, an air-core fiber which supports multiple OAM modes was used to implement a real-time high-dimensional decoy state protocol [24]. Such types of OAM supporting fibers provide an in-line alternative for high-dimensional protocols compared to fibers with multiple cores [25–27].

In QKD, it is important for the transmitted states to be indistinguishable in time, or not to decohere with propagation. Such effects would lead to errors in the obtained measurement outcomes, which cannot be distinguished from the effect of an eavesdropper (Eve) on the quantum link. Thus, the two parties, colloquially named Alice and Bob, would not be able to establish a secure key. On their own, different OAM states of light are distinguishable after propogation through ordinary fibers. One way that these OAM supporting fibers maintain the required indistinguishability is by using a particular set of structured modes of light combining OAM and SAM, the advantage being that these modes could be spatial-division multiplexed with the fundamental mode, which could be encoded with polarization. In this Letter, we present a characterization of one such vortex fiber, and show that it could be used for QKD in a two-dimensional BB84 protocol encoding quantum information on heralded single photons with spatially structured polarization distributions, in addition to encoding in polarization of the fundamental mode. This opens up the possibility to use structured photon fiber networks to increase the classical bandwidth during quantum secure transmission of information.

The vortex fiber used in this Letter is a solid core vortex fiber which supports photons with $\pm\hbar$ units of OAM [17,28], where $\hbar$ is the reduced Planck constant. The operating principle of this type of vortex fiber is that its transverse profile contains a ring of higher refractive index, which resembles the OAM mode shape and acts as a guide for OAM-encoded photons. In additon to having two orthogonal OAM states, photons can simultaneously be either left- or right-handed circularly polarized with $\pm\hbar$ units of SAM. We will write structured photons with the notation $|\ell\rangle_\pi$, where π is the SAM value and ℓ is the OAM value. We will further use the convention that $\pi = +1$ and $\pi = -1$ correspond to left- and right-handed circular polarizations, respectively. In the case of this vortex fiber, the states with the same handedness, $\{|1\rangle_1, |-1\rangle_{-1}\}$, are degenerate in time with each other, i.e., possess identical group velocities in the fiber, but non-degenerate with states of opposite handedness $|1\rangle_{-1}$, $|-1\rangle_1$, and the other fundamental modes of the fiber [29]. Therefore, we take advantage of the states with the same handedness for QKD protocols with this vortex fiber. In particular, for the BB84 protocol, we form two mutually unbiased bases (MUBs), i.e., no information is gained about the states in one basis by making measurements in the other basis, using the aforementioned states, $\mathcal{M}_0 = \{|1\rangle_1, |-1\rangle_{-1}\}$, and $\mathcal{M}_1 = \{(|1\rangle_1 + |-1\rangle_{-1})/\sqrt{2}, (|1\rangle_1 - |-1\rangle_{-1})/\sqrt{2}\}$. This Letter provides a proof-of-concept test that it is feasible to use structured photons, as qubits, through vortex fiber quantum channels which, in principle, can be extended to higher dimensions.

In our experiment (see Fig. 1), we generate heralded single photons via spontaneous parametric downconversion using a 5 mm long periodically poled potassium titanyl phosphate (ppKTP) crystal pumped with a 405 nm diode laser (200 mW). The photon pairs (signal $\lambda_s = 775$ nm and idler $\lambda_i = 850$ nm) are separated via a dichroic mirror (DM), coupled to different single-mode fibers (SMFs). We herald our single photons by detecting the partner photon at an avalanche photodiode (APD) with a dark count rate of less than 50 Hz, which triggers a coincidence counter. The single photon, on which we will imprint information, is first sent to a pair of diffraction gratings and a slit that acts as a narrow bandpass filter, not shown in Fig. 1. A first diffraction grating and lens perform a Fourier transform so that the spectrum is given at the focus. A moveable slit with an adjustable slit width can thus be placed at the focus to precisely choose the desired wavelength and bandwidth. A wavelength of approximately 775 ± 0.75 nm is chosen for the signal photon, since the fiber was designed to operate at this wavelength. A second lens and diffraction grating perform the inverse transformation to recombine the frequencies, subsequently coupled back into SMFs. This adjustable filter is approximately 10% efficient. With a 5 ns coincidence window, our heralded single-photon source has a rate of approximately 4500 coincidences per second after the filter. However, we note that this is not a fundamental constraint, rather a technical deficiency of our setup.

In the preparation stage, Alice prepares the signal photon into a state from either $\mathcal{M}_0$ or $\mathcal{M}_1$ using a sequence of wave plates and a patterned liquid crystal device known as a q-plate, where $q = \ell/2$ is the topological charge of the liquid crystals. Such a device coherently couples SAM to OAM [30,31]. To generate structured photons with $|\ell| = 1$, a $q = 1/2$ plate is utilized, which naturally produces states with the opposite handedness; a half-wave plate is placed after the q-plate to create states with the same handedness, such as in $\mathcal{M}_0$ and $\mathcal{M}_1$. The theoretical phase and polarization distributions of each state are displayed in Fig. 2(a). We note that the modes in MUB $\mathcal{M}_0$ possess uniformly circular polarization distributions, whereas the superposition MUB $\mathcal{M}_1$ consists of spatially varying polarization distributions of only linear polarizations, i.e., structured modes of light. In order to compensate for birefringent coupling induced by the fiber, a set of compensation wave plates [29,32] (not shown in Fig. 1), consisting of two

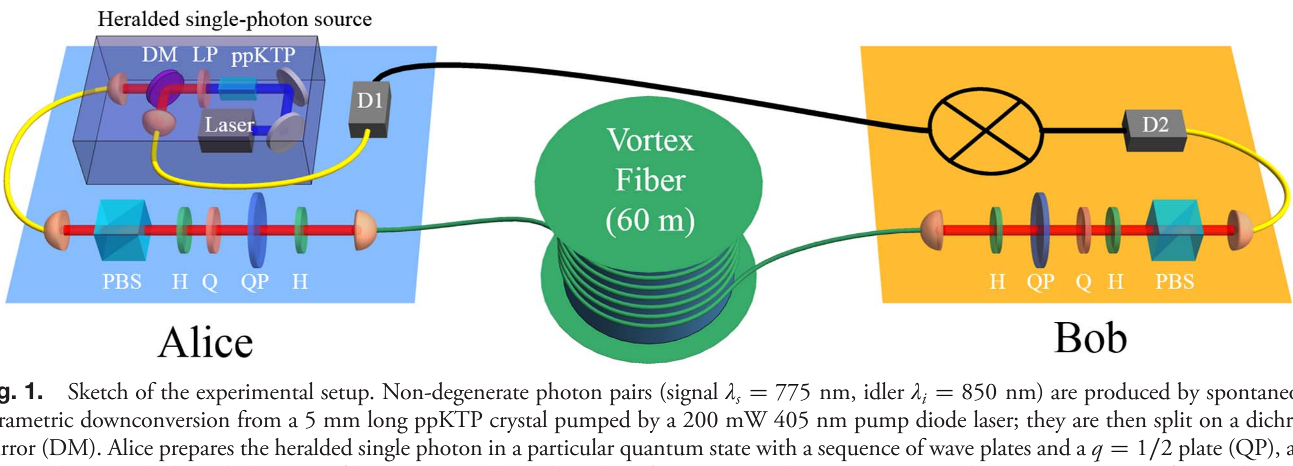

Fig. 1. Sketch of the experimental setup. Non-degenerate photon pairs (signal $\lambda_s = 775$ nm, idler $\lambda_i = 850$ nm) are produced by spontaneous parametric downconversion from a 5 mm long ppKTP crystal pumped by a 200 mW 405 nm pump diode laser; they are then split on a dichroic mirror (DM). Alice prepares the heralded single photon in a particular quantum state with a sequence of wave plates and a $q = 1/2$ plate (QP), and then sends it to Bob through the vortex fiber (quantum channel). Bob performs a particular measurement with a reverse sequence of wave plates and $q = 1/2$ plate, recording a coincidence event between the result (D2) and the heralding trigger photon (D1). H, half-wave plate; Q, quarter-wave plate; LP, long-pass filter; PBS, polarizing beam splitter.

half-wave and two quarter-wave plates, is placed before Alice's q-plate in order to have control of the relative phases between the states in $\mathcal{M}_0$ and $\mathcal{M}_1$.

The structured photons that Alice creates are then coupled into a 60 m long vortex fiber, acting as the untrusted quantum channel, and sent to Bob. There are approximately 50% losses after coupling to the vortex fiber. Bob's setup is similar to Alice's with a mirror sequence of wave plates and $q = 1/2$ plate. A subsequent coupling into an SMF and a detection by an APD enables Bob to project the single photons onto one of the four possible states from the two MUBs, because his system acts as a mode filter: if Bob projected onto the same state as the one Alice sent, then his wave plates and q-plate phase-flatten the mode back to the fundamental, which exclusively couples to the SMF. Bob records the coincidence events between the measured results and the heralding trigger photon at the coincidence logic box. Overall, the system is approximately 9% efficient, with several hundred heralded single photons per second detected after passing through the experimental setup.

We first test the OAM mode propagation through the vortex fiber using a simulator laser diode at 808 ± 0.5 nm by comparing the modes before and after the vortex fiber. Though slightly above the operating wavelength of the fiber, the difference in results should be negligible. The experimentally measured spatial polarization distributions, shown in Figs. 2(b) and 2(c), respectively, were reconstructed using polarization tomography [33]. This is achieved by projecting the transmitted modes onto horizontal, vertical, diagonal, anti-diagonal, left-hand circular, and right-hand circular polarizations using a quarter-wave plate, half-wave plate, and polarizing beam splitter. The six resulting intensity distributions, recorded with a CCD, are used to calculate the Stokes parameters at each point in the mode, thus reconstructing the experimental spatial polarization distribution. A first visual inspection shows that modes after the vortex fiber still resemble the modes that were sent in. By calculating the overlap between the theoretical and experimental polarization distributions, average fidelities of the modes before and after the vortex fiber are $98.8\% \pm 0.3\%$ and $93\% \pm 2\%$, respectively.

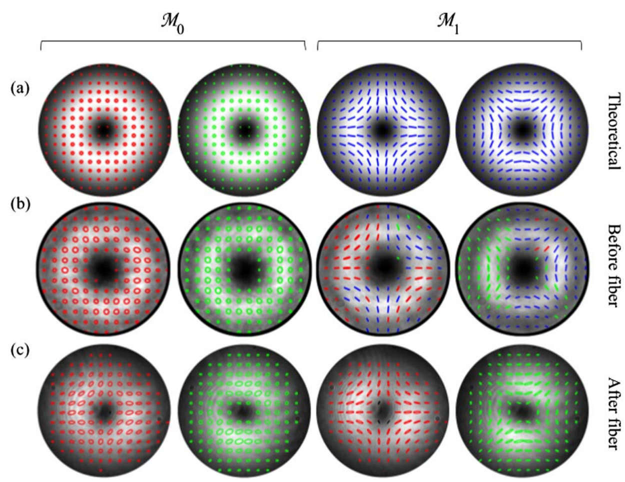

Fig. 2. Intensity (grayscale image) and polarization (overlaid colored pattern) distributions of the vortex fiber modes: (a) theoretical representation, experimentally reconstructed distributions (b) before and (c) after the vortex fiber. The states in MUBs $\mathcal{M}_0$ and $\mathcal{M}_1$ are shown in the first two and last two columns, respectively. The ellipses are colored according to handedness (left-handed = green; right-handed = red); linear states are colored blue, with a tolerance of being 10% elliptically polarized for the experimental plots.

Next, we characterize our vortex fiber more quantitatively as a quantum channel for QKD by methodically generating each state from $\mathcal{M}_0$, $\mathcal{M}_1$, and projecting them onto each state from $\mathcal{M}_0$, $\mathcal{M}_1$. The resulting normalized heralded single-photon counts form a probability-of-detection matrix. The experimental probability-of-detection matrices for the two MUBs, $\mathcal{M}_0$ and $\mathcal{M}_1$, in dimension 2 are shown in Fig. 3(a). In the BB84 protocol with qubits, such as here, the maximum tolerable quantum bit error rate (QBER) threshold, below which a positive secret key rate is produced, is $Q^{\text{th}} = 11\%$. We measured the QBER, calculated as the average of the errors after sifting, to be $Q^{|\ell|=1} = 8.6\%$, which is below the threshold. The secret key rate per sifted photon can be calculated from the QBER as $R(Q) = 1 - 2h(Q)$, where $h(\cdot)$ is the Shannon entropy in dimension 2. Our corresponding secret key rate is 0.15 bits per sifted photon.

We can see from the measurements that when Alice and Bob choose different bases there is crosstalk between the different modes. This is reflected in the mode profiles after propagation through the fiber, giving rise to asymmetric intensity profiles and elliptical polarization distributions in Fig. 2. These errors in the mode structure caused by intermodal coupling in the fiber correspond to a higher QBER, thus requiring more post-processing, such as error correction and privacy amplification [34], leading to lower key rates. However, as stated earlier the vortex fiber also allows for simultaneous performing of polarization-only encoding using a BB84 protocol via spatial-division multiplexing and by encoding the fundamental mode of the fiber, i.e., $\ell = 0$. The MUBs in this case are defined to be $\mathcal{M}_0' = \{|0\rangle_1, |0\rangle_{-1}\}$ and $\mathcal{M}_1' = \{(|0\rangle_1 + |0\rangle_{-1})/\sqrt{2}, (|0\rangle_1 - |0\rangle_{-1})/\sqrt{2}\}$. The measured probability-of-detection matrix is shown in Fig. 3(b). The corresponding QBER of this polarization BB84 scheme is $Q^{\ell=0} = 1.2\%$, with a secret key rate of 0.81 bits per sifted photon. This possibility for multiplexing enables the parallel transmission of more information. An interferometer which sorts based on the total angular momentum of the state [35], or a generalized angular momentum sorter [36], could be used to demultiplex the modes efficiently.

In conclusion, in this Letter, we have explored how structured photons could be used to implement QKD within an

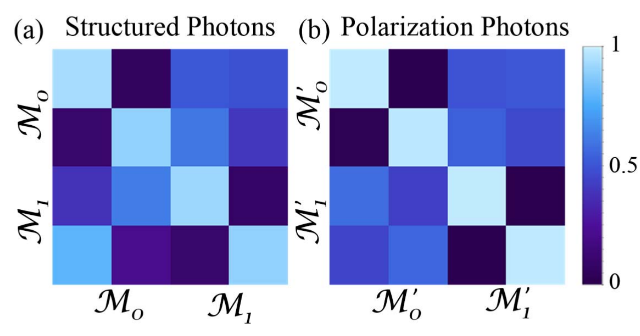

Fig. 3. Experimental probability-of-detection matrices for BB84 schemes using (a) structured photons and (b) polarization. The labels on the left and bottom of the matrix represent the states sent by Alice and projected on by Bob, respectively. QBERs of $Q^{|\ell|=1} = 8.6\%$ and $Q^{\ell=0} = 1.2\%$ are measured for the cases of structured and polarization photons, respectively.

OAM-conserving vortex fiber in a proof-of-concept experiment. The vortex fiber used conserves OAM of $|\ell| = 1$, and modes with the same handedness for both OAM and SAM are indistinguishable with propogation in the fiber; thus, they can serve as additional quantum channels. The obtained QBER rates for the encoding using structured photons, as well as polarization-only encoded photons, are below the theoretical threshold in two dimensions for BB84 and, as such, can be used for establishing a secure key between two parties that are 60 m apart. Although this distance might seem rather short at first sight, network structures within buildings or server infrastrcutures could benefit already from these shorter distances. Future investigations would include studying how errors scale with fiber length and new fibers that support more values of ℓ so that high-dimensional QKD protocols could be employed [12,37]. These types of fibers could create high-dimensional quantum fiber networks, in conjunction with other modes of the fiber, such as the fundamental, which could increase the transmission bandwidth and tolerable error thresholds for more robust and secure quantum communications.

Funding. Natural Sciences and Engineering Research Council of Canada (NSERC); Canada Research Chairs; Canada Excellence Research Chairs, Government of Canada (CERC); Canada Foundation for Innovation (CFI); National Science Foundation (NSF) (ECCS-1610190); Office of Naval Research (ONR) (N00014-13-1-0627).

REFERENCES

1. C. H. Bennett and G. Brassard, in *Proceedings of the International Conference on Computers, Systems and Signal Processing*, Bangalore, India (1984), Vol. **175**, p. 8.
2. J. Yin, Y. Cao, Y.-H. Li, S.-K. Liao, L. Zhang, J.-G. Ren, W.-Q. Cai, W.-Y. Liu, B. Li, H. Dai, G.-B. Li, Q.-M. Lu, Y.-H. Gong, Y. Xu, S.-L. Li, F.-Z. Li, Y.-Y. Yin, Z.-Q. Jiang, M. Li, J.-J. Jia, G. Ren, D. He, Y.-L. Zhou, X.-X. Zhang, N. Wang, X. Chang, Z.-C. Zhu, N.-L. Liu, Y.-A. Chen, C.-Y. Lu, R. Shu, C.-Z. Peng, J.-Y. Wang, and J.-W. Pan, Science **356**, 1140 (2017).
3. J. Yin, Y. Cao, Y.-H. Li, J.-G. Ren, S.-K. Liao, L. Zhang, W.-Q. Cai, W.-Y. Liu, B. Li, H. Dai, M. Li, Y.-M. Huang, L. Deng, L. Li, Q. Zhang, N.-L. Liu, Y.-A. Chen, C.-Y. Lu, R. Shu, C.-Z. Peng, J.-Y. Wang, and J.-W. Pan, Phys. Rev. Lett. **119**, 200501 (2017).
4. J.-G. Ren, P. Xu, H.-L. Yong, L. Zhang, S.-K. Liao, J. Yin, W.-Y. Liu, W.-Q. Cai, M. Yang, L. Li, K.-X. Yang, X. Han, Y.-Q. Yao, J. Li, H.-Y. Wu, S. Wan, L. Liu, D.-Q. Liu, Y.-W. Kuang, Z.-P. He, P. Shang, C. Guo, R.-H. Zheng, K. Tian, Z.-C. Zhu, N.-L. Liu, C.-Y. Lu, R. Shu, Y.-A. Chen, C.-Z. Peng, J.-Y. Wang, and J.-W. Pan, Nature **549**, 70 (2017).
5. S.-K. Liao, W.-Q. Cai, J. Handsteiner, B. Liu, J. Yin, L. Zhang, D. Rauch, M. Fink, J.-G. Ren, W.-Y. Liu, Y. Li, Q. Shen, Y. Cao, F.-Z. Li, J.-F. Wang, Y.-M. Huang, L. Deng, T. Xi, L. Ma, T. Hu, L. Li, N.-L. Liu, F. Koidl, P. Wang, Y.-A. Chen, X.-B. Wang, M. Steindorfer, G. Kirchner, C.-Y. Lu, R. Shu, R. Ursin, T. Scheidl, C.-Z. Peng, J.-Y. Wang, A. Zeilinger, and J.-W. Pan, Phys. Rev. Lett. **120**, 030501 (2018).
6. A. Muller, J. Breguet, and N. Gisin, Europhys. Lett. **23**, 383 (1993).
7. R. Valivarthi, M. G. Puigibert, Q. Zhou, G. H. Aguilar, V. B. Verma, F. Marsili, M. D. Shaw, S. W. Nam, D. Oblak, and W. Tittel, Nat. Photonics **10**, 676 (2016).
8. A. Muller, T. Herzog, B. Huttner, W. Tittel, H. Zbinden, and N. Gisin, Appl. Phys. Lett. **70**, 793 (1997).
9. G. Molina-Terriza, J. P. Torres, and L. Torner, Nat. Phys. **3**, 305 (2007).
10. M. Erhard, R. Fickler, M. Krenn, and A. Zeilinger, Light Sci. Appl. **7**, 17146 (2018).
11. H. Bechmann-Pasquinucci and W. Tittel, Phys. Rev. A **61**, 062308 (2000).
12. N. J. Cerf, M. Bourennane, A. Karlsson, and N. Gisin, Phys. Rev. Lett. **88**, 127902 (2002).
13. H. Rubinsztein-Dunlop, A. Forbes, M. V. Berry, M. R. Dennis, D. L. Andrews, M. Mansuripur, C. Denz, C. Alpmann, P. Banzer, T. Bauer, E. Karimi, L. Marrucci, M. Padgett, M. Ritsch-Marte, N. M. Litchinitser, N. P. Bigelow, C. Rosales-Guzmán, A. Belmonte, J. P. Torres, T. W. Neely, M. Baker, R. Gordon, A. B. Stilgoe, J. Romero, A. G. White, R. Fickler, A. E. Willner, G. Xie, B. McMorran, and A. M. Weiner, J. Opt. **19**, 013001 (2017).
14. M. Mirhosseini, O. S. Magaña-Loaiza, M. N. O'Sullivan, B. Rodenburg, M. Malik, M. P. Lavery, M. J. Padgett, D. J. Gauthier, and R. W. Boyd, New J. Phys. **17**, 033033 (2015).
15. G. Vallone, V. D'Ambrosio, A. Sponselli, S. Slussarenko, L. Marrucci, F. Sciarrino, and P. Villoresi, Phys. Rev. Lett. **113**, 060503 (2014).
16. A. Sit, F. Bouchard, R. Fickler, J. Gagnon-Bischoff, H. Larocque, K. Heshami, D. Elser, C. Peuntinger, K. Günthner, B. Heim, C. Marquardt, G. Leuchs, R. W. Boyd, and E. Karimi, Optica **4**, 1006 (2017).
17. S. Ramachandran, P. Kristensen, and M. F. Yan, Opt. Lett. **34**, 2525 (2009).
18. G. K. L. Wong, M. S. Kang, H. W. Lee, F. Biancalana, C. Conti, T. Weiss, and P. St.J. Russell, Science **337**, 446 (2012).
19. B. Ung, P. Vaity, L. Wang, Y. Messaddeq, L. A. Rusch, and S. LaRochelle, Opt. Express **22**, 18044 (2014).
20. C. Brunet, P. Vaity, Y. Messaddeq, S. LaRochelle, and L. A. Rusch, Opt. Express **22**, 26117 (2014).
21. P. Gregg, P. Kristensen, and S. Ramachandran, Optica **2**, 267 (2015).
22. N. Bozinovic, S. Ramachandran, M. Brodsky, and P. Kristensen, *Frontiers in Optics 2011/Laser Science XXVII* (Optical Society of America, 2011), paper PDPB1.
23. N. Bozinovic, Y. Yue, Y. Ren, M. Tur, P. Kristensen, H. Huang, A. E. Willner, and S. Ramachandran, Science **340**, 1545 (2013).
24. D. Cozzolino, D. Bacco, B. D. Lio, K. Ingerslev, Y. Ding, K. Dalgaard, P. Kristensen, M. Galili, K. Rottwitt, S. Ramachandran, and L. K. Oxenlowe, "Fiber based high-dimensional quantum communication with twisted photons," preprint arXiv:1803.10138 (2018).
25. J. F. Dynes, S. J. Kindness, S. W.-B. Tam, A. W. Sharpe, M. Lucamarini, B. Frölich, Z. L. Yuan, R. V. Penty, and A. J. Shields, Opt. Express **24**, 8081 (2016).
26. G. Cañas, N. Vera, J. Cariñe, P. González, J. Cardenas, P. W. R. Connolly, A. Przysiezna, E. S. Gómez, M. Figueroa, G. Vallone, P. Villoresi, T. F. da Silva, G. B. Xavier, and G. Lima, Phys. Rev. A **96**, 022317 (2017).
27. Y. Ding, D. Bacco, D. Kjeld, X. Cai, X. Zhou, K. Rottwitt, and L. K. Oxenløwe, npj Quantum Inf. **3**, 1 (2017).
28. L. Yan, P. Kristensen, and S. Ramachandran, *Conference on Lasers and Electro-Optics*, OSA Technical Digest 2016 (Optical Society of America, 2016), paper SM4P.3.
29. P. Gregg, M. Mirhosseini, A. Rubano, L. Marrucci, E. Karimi, R. W. Boyd, and S. Ramachandran, Opt. Lett. **40**, 1729 (2015).
30. L. Marrucci, C. Manzo, and D. Paparo, Phys. Rev. Lett. **96**, 163905 (2006).
31. H. Larocque, J. Gagnon-Bischoff, F. Bouchard, R. Fickler, J. Upham, R. W. Boyd, and E. Karimi, J. Opt. **18**, 124002 (2016).
32. R. Bhandari, Phys. Lett. A **138**, 469 (1989).
33. F. Cardano, E. Karimi, S. Slussarenko, L. Marrucci, C. de Lissio, and E. Santamato, Appl. Opt. **51**, C1 (2012).
34. N. Gisin, G. Ribordy, W. Tittel, and H. Zbinden, Rev. Mod. Phys. **74**, 145 (2002).
35. J. Leach, J. Courtial, K. Skeldon, S. M. Barnett, S. Franke-Arnold, and M. J. Padgett, Phys. Rev. Lett. **92**, 013601 (2004).
36. H. Larocque, J. Gagnon-Bischoff, D. Mortimer, Y. Zhang, F. Bouchard, J. Upham, V. Grillo, R. W. Boyd, and E. Karimi, Opt. Express **25**, 19832 (2017).
37. F. Bouchard, K. Heshami, D. England, R. Fickler, R. W. Boyd, B.-G. Englert, L. L. Sánchez-Soto, and E. Karimi, "Experimental investigation of quantum key distribution protocols with twisted photons," preprint arXiv:1802.05773 (2018).